24th ABCM International Congress of Mechanical Engineering
December 3-8, 2017, Curitiba, PR, Brazil

COBEM-2017-0740
MULTIMODAL VIBRATION CONTROL USING DYNAMIC NEUTRALIZERS IN ROTATING MACHINES

Danielle Raphaela Voltolini
WEG Equipamentos Elétricos S.A. – Energy Division, Department of Development and Technological Innovation – Avenida Prefeito Waldemar Grubba, 3300, Vila Lalau – Jaraguá do Sul-SC, Brazil – 89256-900.
danieller@weg.net

Samuel Kluthcovsky
Eduardo Márcio de Oliveira Lopes
Carlos Alberto Bavastri
Universidade Federal do Paraná – Department of Mechanical Engineering – Centro Politécnico, Bloco IV – Setor de Tecnologia, Jardim das Américas – Curitiba-PR, Brazil – 81531-990.
samuelkluth@gmail.com
edumolopes@gmail.com
bavastri@ufpr.br

Abstract. *Rotating machines often work close to or even above their critical speeds, becoming susceptible to resonance or dynamic instability. These phenomena may cause high vibration levels, particularly when rolling bearings are used. Viscoelastic dynamic vibration neutralizers (VDVNs) are relatively cheap passive devices with a wide range of applications, including the vibrations control of rotating systems. These devices can be designed according to specific needs for controlling flexural vibration in dynamic rotors, and the point where the device is attached depends, in some cases, on the mode to be controlled. In electrical motors and generators, for example, with reduced internal space, the position to attach it is an important variable. The current paper focuses on the angular VDVN for shaft slope degree of freedom (DOF) control acting indirectly by reducing multimodal flexural vibrations. The angular VDVN can be installed close to the bearing where the slope DOF presents its highest value at any critical speed and where there is no lack of space. The conceptual design of the angular VDVN is shown to illustrate the proposed methodology, and a numerical example is given to demonstrate the influence of the angular VDVN on the response around the first two critical speeds.*

Keywords: *Angular Vibration Neutralizer, Flexural Vibration Control, Optimal Multimodal Control, Rotordynamics, Viscoelastic Material.*

1. INTRODUCTION

The demand for energy and high efficiency is growing year after year and, therefore, the use of high-speed machines in industrial applications is also growing. As the consequence of this, these machines have been working close or even above their critical speeds, where dynamic instabilities and resonance phenomena may affect the dynamic behavior of the system.

In a system with low damping – like a rotor mounted on rolling bearings – it is practically impossible to operate it above the first critical speed without some sort of vibration control. This problem is usually solved by using hydrodynamic or magnetic bearings, but these solutions are relatively expensive and require a complex auxiliary system to control them. In the case of hydrodynamic bearings, there is a common problem regarding oil leakage and fluid system maintenance.

Recently, Lee *et al.* (2008) developed an experimental analysis to demonstrate, by using a bearing made of viscoelastic material, that it is possible to obtain a dynamic behavior comparable to that of conventional bearings. A dynamic rotor model using viscoelastic supports at the base of rolling bearings, proposed by Bavastri *et al.* (2008) and Ribeiro *et al.* (2015) takes the issue to a new level by establishing an optimal design for supports composed of viscoelastic springs and tuned internal lumps of mass, to reduce vibration levels in rotating systems.

However, high vibration levels may also be controlled using simple devices called ‘viscoelastic dynamic vibration neutralizers’ – or VDVNs for short – whose early applications are described by Snowdon (1959). Doubrawa Filho *et al.* (2010) described a methodology to optimize the design of translational VDVN to control the flexural vibration response acting in displacement degrees-of-freedom (DOFs).

These translational VDVNs must be mounted far from the bearings, because the maximum amplitudes of the flexural vibration modes occur between supports. Although, this may not be possible in some cases – as in electrical motors and generators, as in Fig. 1 below – because the rotor package is mounted in this area, and because the length of machines is becoming smaller and smaller each year.

Figure 1. Example of an electric machine (WEG SM40) lacking inner space to use translational VDVNs.

A new type of neutralizer, called 'angular VDVN', will be presented here. This neutralizer indirectly controls the flexural vibration response by acting on the slope DOF. The angular VDVNs may be mounted close to the bearings, where the slope degree-of-freedom (DOF) is highest, with the advantages of easy maintenance and installation. Using this same attachment point, angular VDVN may control any vibration mode, whereas translational VDVNs are placed according to the vibration mode to be controlled.

This paper focuses on the methodology for an optimal design of angular VDVNs to control two different modes with the same device (multimodal control).

2. MODE SHAPES

Simple rotor geometry, as used in the current paper, may be close to a simply-supported Euler-Bernoulli beam, and its first four vibration modes are represented in Fig. 2.

For any mode, the slope DOF – that is, the angular displacement at a certain point – will be present near the supports. So, if a neutralizer is attached to this position, it may reduce the vibration response of the primary system for any mode since there is a relative displacement between the primary system and the neutralizer.

The same statement is not valid for translational VDVNs because they act on the displacement DOF and, as shown in Fig. 2, except for the first mode, there are modes in which there is no displacement. In this case, the place where the device will be attached is very important, limiting the use of translational VDVNs to a single mode and rendering it inadequate to multimodal control.

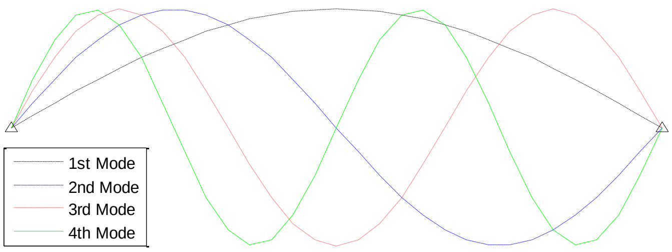

Figure 2. First four modes of an Euler-Bernoulli simply-supported beam.

3. VISCOELASTIC MATERIAL

In the current paper, the vibration dynamic neutralizer is composed of a viscoelastic material, a special polymeric material with complex elasticity moduli function of frequency and temperature. There are some different analytical models to characterize them, but in this paper the four-parameter fractional derivative model – as detailed by Pritz (1996) and Jones (2001) – is chosen, because it can be used in thermorheologically simple materials. In the frequency domain, for a given environmental temperature *T*, the complex shear modulus $\overline{G}(\Omega,T)$ is as follows:

$$\overline{G}(\Omega,T)=\frac{G_0+G_\infty.b_1(i.\Omega.\alpha(T))^\beta}{1+b_1(i.\Omega.\alpha(T))^\beta}=G_r(\Omega,T)(1+i.\eta(\Omega,T)) \quad (1)$$

where, parameters G_0 and G_∞ represent the asymptotic values of the dynamic shear modulus at low and high frequencies, respectively, parameter $b_1=b^\beta$ represents an experimentally determined constant, *b* is the relaxation time, as shown in Pritz (1996), and β is the fractional derivative power. Function $\alpha(T)$ is the shift factor and represents the influence of temperature. Williams, Landel, and Ferry – as shown in Ferry (1980) – proposed a model for this factor, resulting in the so-called 'WLF equation':

$$log\,\alpha(T)=-\theta_1\frac{(T-T_0)}{(\theta_2+(T-T_0))} \quad (2)$$

where constants θ_1 and θ_2 may be determined experimentally, parameter T_0 is an arbitrary reference temperature, and *T* is the working temperature, both in Kelvin.

In Eq. (1), $G_r=Re(\overline{G}(\Omega))$ is the dynamic shear modulus which is defined as the real part of the complex shear modulus, $\eta(\Omega)=Im(\overline{G}(\Omega))/Re(\overline{G}(\Omega))$ is the loss factor expressed by the relationship between the imaginary and real parts of the complex shear modulus. There is an analogous expression to Eq. (1) for the complex Young's modulus $\overline{E}(\Omega,T)$.

In order to simplify notation, parameter *T* will be suppressed from now on because the neutralizer will be designed for a specific working temperature.

4. ROTATING SYSTEM

As presented by Genta (2005), the linearized equation of motion below is applicable to "a linear rotor that is axially symmetrical around its spin axis and rotates at a constant spin speed *Ω"*.

$$[M]\{\ddot{q}(t)\}+([C]+[G])\{\dot{q}(t)\}+([K]+[H])\{q(t)\}=\{f(t)\} \quad (3)$$

where $\{q(t)\}$ is the generalized coordinate vector, $[M]$ is the symmetrical mass matrix, $[C]$ is the symmetrical damping matrix, $[K]$ is the symmetrical stiffness matrix, $[G]$ is the skew-symmetrical gyroscopic matrix, $[H]$ is the skew-symmetrical circulatory matrix, and $\{f(t)\}$ is the time-dependent vector for forcing functions. In the current paper, the circulatory matrix will be disregarded; so, in the frequency domain, Eq. 3 is expressed by

$$\left(-\Omega^2[M]+i\Omega([C]+[G(\Omega_{rpm})])+[K]\right)\{Q[\Omega]\}=\{F(\Omega)\} \quad (4)$$

Transforming Eq. 4 to space state, as shown by Genta (2005), it is possible to solve the motion equation by addressing the associated eigenvalue problem and its adjoint counterpart, for a fixed rotation, Ω_{rpm}.

5. COMPOUND SYSTEM – CONTROL DESIGN

The translational VDVN may be represented by a single lumped mass *(m)* connected to a rigid massless base through a resilient viscoelastic device (Fig. 3a) with complex stiffness $L\overline{G}(\Omega)$, as presented by Espíndola and Silva (1992).

Espíndola *et al.* (2010) present the generalized equivalent parameters, where the system is represented by an equivalent mass $(m_e(\Omega))$ and an equivalent viscous damping $(c_e(\Omega))$ (Fig. 3b). The equivalent viscous damping is defined as the real part of the mechanical impedance at the base of the neutralizer, and the equivalent generalized mass is the real part of the dynamic mass.

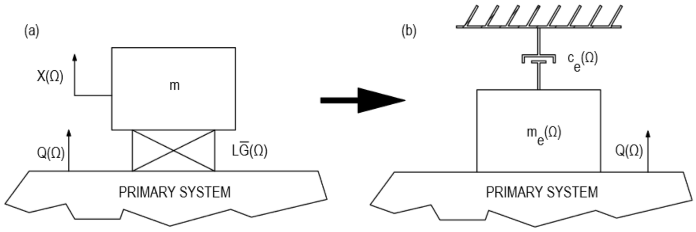

Figure 3. (a) Simple system with translational VDVN and (b) its equivalent compound system.

Based on this, it is possible to apply this concept to a slope DOF system, as shown in Fig. 4, where the translational dynamic stiffness is replaced by the angular dynamic stiffness $\bar{K}_{bs}(\Omega)$, and it is expressed by the relation between an external moment applied to its base *($M_b(\Omega)$)* and the slope DOF at the same point *($\theta_b(\Omega)$)* (Fig. 5).

$$\bar{K}_{bs}(\Omega)=\frac{M_b(\Omega)}{\theta_b(\Omega)}=-\Omega^2 m_{es}(\Omega)+i\Omega c_{es}(\Omega) \tag{5}$$

where $m_{es}(\Omega)$ and $c_{es}(\Omega)$ are the generalized equivalent parameters of mass and damping, respectively. They are obtained by comparing the real and the imaginary parts of the angular dynamic stiffness.

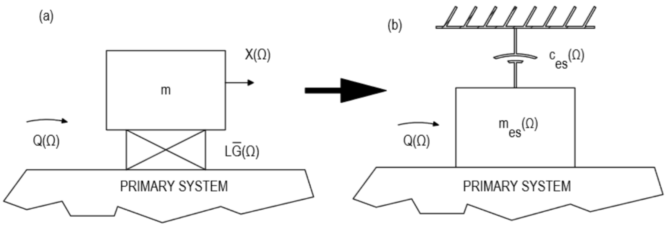

Figure 4. (a) Simple system with angular VDVN and (b) its equivalent compound system.

The external moment is found by applying the free body diagram and Newton's second law to the simplified model shown in Fig. 5:

$$\begin{cases} M_b(\Omega)-F_R(\Omega)R=-\Omega^2 I_b\theta_b(\Omega) \\ F_R(\Omega)R=-\Omega^2 I\theta(\Omega) \end{cases} \tag{6}$$

where $F_R(\Omega)$ is the lateral reaction force, R is the distance between the shaft centerline and the center of viscoelastic material element, I_b is the inertia moment of the base, I is the inertia moment of the mass, and $\theta(\Omega)$ is the slope DOF of the mass. On the other hand, $F_R(\Omega)$ is given by $F_R(\Omega)=\bar{K}(\Omega)(X_b(\Omega)-X(\Omega))=L\bar{G}(\Omega)(X_b(\Omega)-X(\Omega))$, where $\bar{K}(\Omega)$ is the complex stiffness, which is composed of the complex shear modulus $\bar{G}(\Omega)$ and a form factor L. This form factor is expressed by the relationship between the shear area, A, and the thickness of the viscoelastic material, h. Variables $X_b(\Omega)$ and $X(\Omega)$ are the displacements at the base and the mass of the neutralizer, respectively, and are, approximately:

$$\begin{aligned} X_b(\Omega)&=\theta_b(\Omega)(R-h/2)\approx\theta_b(\Omega)R \\ X(\Omega)&=\theta(\Omega)(R+h/2)\approx\theta(\Omega)R \end{aligned} \tag{7}$$

The dynamic stiffness at the base of the neutralizer can be found by combining Eq. 6 and 7 in such a way that:

$$\bar{K}_{bs}(\Omega)=\frac{M_b(\Omega)}{\theta_b(\Omega)}=\frac{-\Omega^2 L\bar{G}(\Omega)R^2(I+I_b)+\Omega^4 II_b}{-\Omega^2 I+L\bar{G}(\Omega)R^2} \tag{8}$$

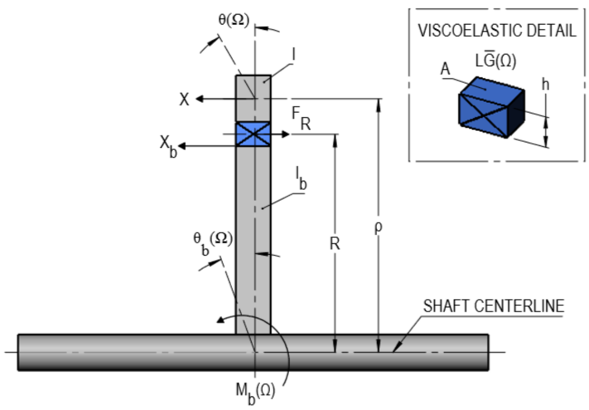

Figure 5. Simplified model for angular VDVN.

Using Eq. 8 and multiplying the right side by $(1/G_r(\Omega_n))/(1/G_r(\Omega_n))$, where $G_r(\Omega_n)$ is the real part of complex shear modulus calculated at the natural frequency Ω_n, it is possible to obtain the dynamic equivalent mass $m_{es}(\Omega)$ and the dynamic equivalent stiffness $c_{es}(\Omega)$, as shown in the second part of Eq. 5:

$$m_{es}(\Omega)=\frac{r(\Omega)R^2(I+I_b)\left[-\varepsilon(\Omega)^2+r(\Omega)R^2\left(1+\eta(\Omega)^2\right)\right]-\varepsilon(\Omega)^2 I_b\left[-\varepsilon(\Omega)^2+r(\Omega)R^2\right]}{\left[-\varepsilon(\Omega)^2+r(\Omega)R^2\right]^2+r(\Omega)^2\eta(\Omega)^2R^4} \tag{9}$$

$$c_{es}(\Omega)=\frac{\Omega r(\Omega)R^2\eta(\Omega)\varepsilon(\Omega)^2 I}{\left[-\varepsilon(\Omega)^2+r(\Omega)R^2\right]^2+r(\Omega)^2\eta(\Omega)^2R^4} \tag{10}$$

where $r(\Omega)= LG_r(\Omega)/ LG_r(\Omega_n)$, $\Omega_n^2= LG_r(\Omega_n)/m$ and $\varepsilon(\Omega)=\Omega/\Omega_n$.

Equalizing the denominator of Eq. 8 to zero, it is possible to obtain the control frequency, Ω_θ, which is:

$$\Omega_\theta=\sqrt{\frac{LG_r(\Omega_n)R^2}{I}} \tag{11}$$

Once the inertia $I\approx m\rho^2$, where ρ is the radial distance between the rotor centerline and the center of the mass, the relationship between Ω_n and Ω_θ is:

$$\Omega_\theta=\Omega_n\frac{R}{\rho} \tag{12}$$

Analyzing Eq. 12 and Fig. 5, $R<\rho$, then $\Omega_\theta<\Omega_n$. So, the neutralizer natural frequency Ω_θ can be obtained in such a way that it is as low as necessary.

Based on this, it is possible to add the equivalent mass and damping introduced by the angular VDVNs into the primary system as:

$$[C_e(\Omega)]=\begin{bmatrix}0&0&\cdots&0&0\\0&c_{es_1}(\Omega)&\cdots&0&0\\\vdots&\vdots&\ddots&\vdots&\vdots\\0&0&\cdots&c_{es_p}&0\\0&0&\cdots&0&0\end{bmatrix};[M_e(\Omega)]=\begin{bmatrix}0&0&\cdots&0&0\\0&m_{es_1}(\Omega)&\cdots&0&0\\\vdots&\vdots&\ddots&\vdots&\vdots\\0&0&\cdots&m_{es_p}(\Omega)&0\\0&0&\cdots&0&0\end{bmatrix}\begin{matrix}\vdots\\\leftarrow\theta_{j1}\\\vdots\\\leftarrow\theta_{jp}\\\vdots\end{matrix} \tag{13}$$

where parameters c_{esj} and m_{esj} correspond to the j^{th}, with $j=1$ to p, angular VDVNs.

Based on this, Eq. 4 for the compound system is:

$$\left[-\Omega^2([M]+[M_e(\Omega)])+i\Omega([C]+[C_e(\Omega)]+[G(\Omega_r)]+[K])\right]\{Q(\Omega)\}=\{F(\Omega)\} \tag{14}$$

The associated eigenvalue problem and its adjoint counterpart must be resolved in order to obtain the solution in modal or sub-modal state space.

6. OPTIMIZATION

The design of angular VDVNs is possible by using an optimization algorithm, and its aim is to obtain the optimal natural frequency for the VDVN. The first step in solving the standard optimization problem is to calculate the general equivalent parameters of Eq. 9 and Eq. 10 and solve the motion equation shown in Eq. 14. Then, the composite system response values in the modal primary system state space *($P(\Omega)$)* – as shown in Doubrawa Filho *et al.* (2010) – are evaluated in the objective function *(f_{obj})*:

$$f_{obj}(x)=\left\| \max_{\Omega < \Omega < \Omega_2} \left| P(\Omega,x) \right| \right\| \quad (15)$$

where x is the design vector containing the natural frequencies of the neutralizer ($x^T=[\Omega_{a1}, \Omega_{a2}, \ldots, \Omega_{ap}]$), parameters Ω_1 and Ω_2 represent the frequency band of control (related to rotating speeds), and may be determined based on the rotordynamics analysis for flexural modes. The *'max'* reference indicates the maximum value for each component of the $P(\Omega,x)$ vector, in the frequency band of interest, for a given design vector, in a modal subspace of the primary system; and $\| \; \|$ is the Euclidian norm.

The resolution of the optimization problem uses standard barrier functions to ensure convergence, and they are inequality constraints defined by $\Omega_{ai}^L<\Omega_{ai}>\Omega_{ai}^U$, with $i=1$ *to* p, L and U are lower and upper constraints, respectively.

In addition to the optimal natural frequencies, the design of angular VDVNs needs the inertial mass, and Espíndola and Silva (1992) define it for a mode-to-mode control. The following relation (μ_j) between the inertial mass of the neutralizers and the modal inertial of the primary system is used:

$$\mu_j = \frac{I_a \sum_{s=1}^{p} \left| \varphi_{k_s j} \right|^2}{I_j} \quad (16)$$

where I_a is the mass moment of inertia of the neutralizers, I_j is the modal mass moment of inertia of the primary system and φ_{ksj} is the (k_s,j) elements of the right modal matrix in the state space. Parameter k_s represents the position where the i^{th} neutralizer is attached with $s=1$ to p, p is the number of neutralizers, and j is the j^{th} mode to be controlled. The relation μ_j takes on typical values between 0.1 and 0.25.

Equation 16 provides the inertial mass of the neutralizer, and it may be approximately determined from the product between the mass and the square length of the arm (ρ).

7. CASE STUDY, PARAMETERS, AND DISCUSSION

7.1 Numerical Model

To analytically validate the methodology presented above, the following rotor geometry was selected. This model was based on a real geometry of an experimental rotor placed on the Laboratory of Vibrations and Sound – UFPR. The experiment used one shaft with 25 mm diameter and 1 m length made of steel with 207 GPa Young Modulus, 0.3 Poisson coefficient and 7850 kg/m³ density. Two steel discs (7850 kg/m³ density) were also used: the first positioned 458 mm from the origin, 130 mm external diameter, and 30 mm length; the second positioned 980 mm from the origin, 180 mm external diameter, and 30 mm length. The bearings are positioned 47 mm and 800 mm away from origin, and they have the same stiffness in directions x-x and z-z, 1e9 N/m, and without stiffness in the cross-directions x-z and z-x. The damping used for the bearings was 500 N.s/m in direction x-x and z-z, and without damping in cross-directions x-z and z-x. The model is shown in Fig. 6.

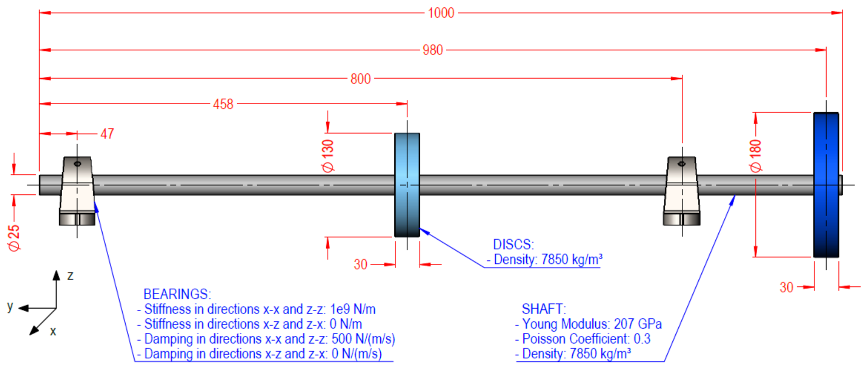

Figure 6. Rotor geometry (dimensions in mm).

The unbalance excitation with 2e-4 kg.m was added to the model at 458 mm position (right in the middle of the first disc), as shown in the finite-element model of Fig. 7. The excitation node chosen was 11 and the evaluation node was 3 (near the bearing).

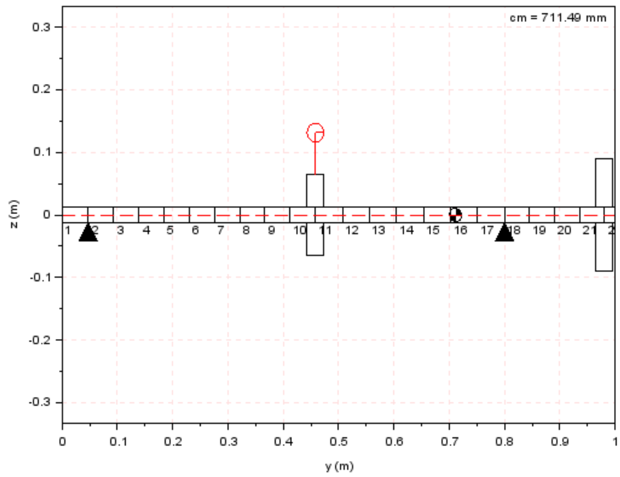

Figure 7. Finite-element model used to characterize rotor system.

The butyl rubber viscoelastic material used was code BT-806/55 and its parameters are: $T_0 = 243$ K, $G_0 = 2.4$ MPa, $G_\infty = 152.3$ MPa, $\beta = 0.417$, $b_1 = 0.0223$, and the temperature constants $\theta_1 = 7.98$ and $\theta_2 = 81.7$. The selected working temperature was 23 ºC. The corresponding nomogram of butyl rubber is presented in Fig. 8.

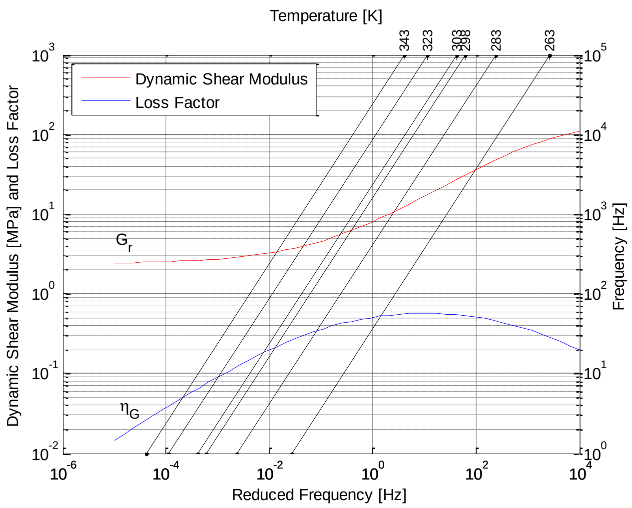

Figure 8. Nomogram of butyl rubber.

The angular VDVN was placed at node 19 (Fig. 7). Two different configurations were used: first mode control and second mode control. The parameters for inertia, initial frequency for optimization routine and barriers are the following:

- **First mode control:**
  - *Initial frequency:* 32 Hz;
  - *Barriers (bottom and upper):* 25 Hz and 65 Hz;
  - *Inertia:* 3.9154e-2 kg.m²;
- **Second mode control:**
  - *Initial frequency:* 80 Hz;
  - *Barriers (bottom and upper):* 58 Hz and 98 Hz;
  - *Inertia:* 3.9172e-2 kg.m²;

7.2 Results and Discussions

The unbalance response for primary system without neutralizer is shown in blue dashed-dotted line in Fig.9, and the first four critical speeds are 1905, 2084, 4708, and 5093 rpm. The compound system (primary system plus neutralizer) is represented by black and red lines. The black solid line is the unbalance response with the neutralizer tuned to first mode, and the optimum frequency of the neutralizer is 43.4 Hz. However, the red dashed line is also the unbalance response, but for the compound system with the neutralizer tuned to second mode, the optimum frequency is 73.3 Hz. The optimum frequencies of the neutralizers are presented in Tab. 1.

Table 1. Optimum frequencies for the cases.

	Optimum Frequency
First mode control	$f_{1m}=43.3\ Hz$
Second mode control	$f_{2m}=73.3\ Hz$

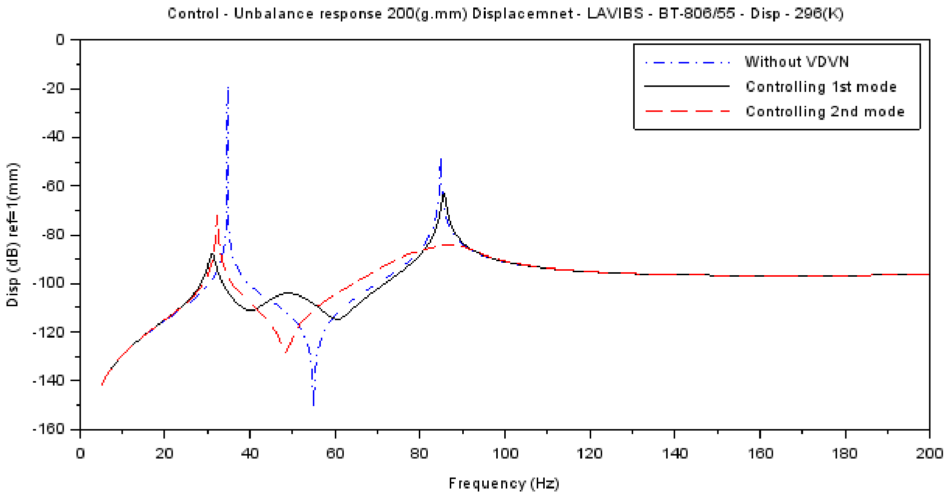

Figure 9. Unbalance response without neutralizers and with neutralizers controlling the 1st and 2nd modes.

Analyzing the unbalance responses shown in Fig. 9, it is possible to note that both cases result in substantial reduction in unbalance response (UR), as summarized in Tab. 2.

Table 2. Summary: reduction of unbalance response.

	Controlling 1st mode	Controlling 2nd mode
UR – 1st mode	Reduction of 70dB	Reduction of 50dB
UR – 2nd mode	Reduction of 15dB	Reduction of 40dB

Based on Tab. 2, it is difficult to choose the best way to design the angular VDVN, but in what concerns the physical construction of the device, the higher the designed natural frequency, the greater the form factor will be (L –Eq. 11) for the neutralizer, and consequently, the dimensions of the viscoelastic material will also be greater. The larger the viscoelastic blanket, or the shear area, the easier its manipulation and manufacturing will be.

8. CONCLUSION

The methodology to design optimal angular VDVNs to reduce flexural vibration levels in rotating machines was introduced and implemented.

To demonstrate the capacity of multimodal control by using the angular VDVNs, an example was presented.

In the current paper, two different cases were presented: one of them to control first mode and the other to control the second mode. Regarding the reduction of the unbalance response, both presented promising results, but the second case can be considered better than the first, because the natural frequency obtained is the highest. This is desirable due the facility to build a device with greater shear area, which implicates a greater viscoelastic segment.

9. ACKNOWLEDGEMENTS

Danielle Raphaela Voltolini acknowledges the support from the WEG Group.

Eduardo Márcio de Oliveira Lopes and Carlos Alberto Bavastri gratefully acknowledge the financial support of CNPq – Brazil's National Council for Scientific and Technological Development.

10. REFERENCES

Bavastri, C.A., Ferreira, E.M.S., Espíndola, J.J. and Lopes, E.M. de O., 2008. "Modeling of Dynamic Rotors with Flexible Bearings due to the use of Viscoelastic Materials". In *Journal of the Brazilian Society of Mechanical Sciences and Engineering*, 30(1): 22-29.

Doubrawa Filho, F.J., Luersen, M.A. and Bavastri, C.A., 2010. "Optimal design of viscoelastic vibration absorbers for rotating systems". In *Journal of Vibration and Control*, 17(5): 699-710.

Espíndola, J.J., Bavastri, C.A., Lopes, E.M.O., 2010. "On the Passive Control of Vibrations with Viscoelastic Dynamic Absorbers of Ordinary and Pendulum Types". In *Journal of the Franklin Institute*, 347(1): 102-115.

Espíndola, J.J., Silva, H.P., 1992. "Modal reduction of vibrations by dynamic nuetralizers: a generalized approach". In *IMAC-10 – 10th Internatiocal Modal Analysis Conference. Society for Experimental Mechanics*, 2: 1367-1373.

Ferry, J.D., 1980. *Viscoelastic Properties of Polymers*. John Wiley & Sons, 3rd edition.

Genta, G., 2005. *Dynamics of Rotating Systems.* Springer-Verlag, New York.

Jones, D.I.G., 2001. *Handbook of Viscoelastic Vibration Damping*. John Wiley & Sons.

Lee, Y., Kim, T., Kim, C., Lee, N., Choi, D., 2004. "Dynamic characteristics of a flexible rotor system supported by a viscoelastic foil bearing (VEFB)". In *Tribology International*, 37: 679-687.

Pritz, T., 1996. "Analysis of four-parameter fraction derivative model of real solid materials". In *Journal of Sound and Vibration*, 195(1): 103-115.

Ribeiro, E.A., Pereira, J.T. and Bavastri, C.A., 2015. "Passive vibration control in rotor dynamics: Optimization of composed support using viscoelastic materials". In *Journal of Sound and Vibration*, 351(1): 43-56.

Snowdon, J.C., 1959. "Steady-state behavior of the dynamic absorber". In *Journal of Acoustical Society of America*, 38: 1096-1103.

11. RESPONSIBILITY NOTICE

The authors are the only responsible for the printed material included in this paper.